

University of Dundee

GDF15 mediates the effects of metformin on body weight and energy balance

Coll, Anthony P.; Chen, Michael; Taskar, Pranali; Rimmington, Debra; Patel, Satish; Tadross, John

Published in:
Nature

DOI:
[10.1038/s41586-019-1911-y](https://doi.org/10.1038/s41586-019-1911-y)

Publication date:
2020

Document Version
Peer reviewed version

[Link to publication in Discovery Research Portal](#)

Citation for published version (APA):

Coll, A. P., Chen, M., Taskar, P., Rimmington, D., Patel, S., Tadross, J., Cimino, I., Yang, M., Welsh, P., Virtue, S., Goldspink, D. A., Miedzybrodzka, E. L., Konopka, A. R., Ruiz Esponda, P., Huang, J., Tung, Y. C. L., Rodriguez-Cuenca, S., Tomaz, R. A., Harding, H. P., ... O'Rahilly, S. P. (2020). GDF15 mediates the effects of metformin on body weight and energy balance. *Nature*, 578, 444-448. <https://doi.org/10.1038/s41586-019-1911-y>

General rights

Copyright and moral rights for the publications made accessible in Discovery Research Portal are retained by the authors and/or other copyright owners and it is a condition of accessing publications that users recognise and abide by the legal requirements associated with these rights.

- Users may download and print one copy of any publication from Discovery Research Portal for the purpose of private study or research.
- You may not further distribute the material or use it for any profit-making activity or commercial gain.
- You may freely distribute the URL identifying the publication in the public portal.

Take down policy

If you believe that this document breaches copyright please contact us providing details, and we will remove access to the work immediately and investigate your claim.

1 **GDF15 mediates the effects of metformin on body weight and energy balance**

2 Anthony P Coll^{1&*}, Michael Chen², Pranali Taskar², Debra Rimmington¹, Satish
3 Patel¹, JohnTadross¹, Irene Cimino¹, Ming Yang¹, Paul Welsh³, Samuel Virtue¹,
4 Deborah A. Goldspink¹, Emily L. Miedzybrodzka¹, Adam R Konopka⁴, Raul Ruiz
5 Esponda⁴, Jeffrey T.-J. Huang⁵, Y. C. Loraine Tung¹, Sergio Rodriguez-Cuenca¹,
6 Rute A. Tomaz⁶, Heather P. Harding⁷, Audrey Melvin¹, Giles S.H. Yeo¹, David
7 Preiss⁸, Antonio Vidal-Puig¹, Ludovic Vallier⁶, K. Sreekumaran Nair⁴, Nicholas J.
8 Wareham⁹, David Ron⁷, Fiona M. Gribble¹, Frank Reimann¹, Naveed Sattar^{3&}, David
9 B. Savage^{1&}, Bernard B. Allan^{2&}, Stephen O'Rahilly^{1&*}

10 * correspondence to apc36@cam.ac.uk or so104@medschl.cam.ac.uk

11 & These authors contributed equally to this work.

12 1. MRC Metabolic Diseases Unit, Wellcome Trust-Medical Research Council
13 Institute of Metabolic Science, University of Cambridge, Cambridge CB2 0QQ, UK

14 2. NGM Biopharmaceuticals, South San Francisco, California 94080, USA

15 3. Institute of Cardiovascular and Medical Sciences, University of Glasgow,
16 Glasgow.

17 4. Division of Endocrinology, Mayo Clinic, Rochester, MN 55905, USA

18 5. Division of Systems Medicine, School of Medicine, University of Dundee, Dundee,
19 DD1 9SY

20 6. Wellcome -Medical Research Council Cambridge Stem Cell Institute, Anne
21 McLaren Laboratory for Regenerative Medicine, University of Cambridge,
22 Cambridge, UK.

23 7. Cambridge Institute for Medical Research, University of Cambridge, Cambridge
24 CB2 0XY, UK

25 8. MRC Population Health Research Unit, Clinical Trial Service Unit and
26 Epidemiological Studies Unit, Nuffield Department of Population Health, University of
27 Oxford, UK.

28 9. MRC Epidemiology Unit, Wellcome Trust-Medical Research Council Institute of
29 Metabolic Science, University of Cambridge, Cambridge, UK.

30 **Metformin, the world's most prescribed anti-diabetic drug, is also effective in**
31 **preventing Type 2 diabetes in people at high risk^{1,2}. Over 60% of this effect is**
32 **attributable to metformin's ability to lower body weight in a sustained manner³.**
33 **The molecular mechanisms through which metformin lowers body weight are**
34 **unknown. In two, independent randomised controlled clinical trials,**
35 **circulating levels of GDF15, recently described to reduce food intake and lower**
36 **body weight through a brain stem-restricted receptor, were increased by**
37 **metformin. In wild-type mice, oral metformin increased circulating GDF15 with**
38 ***GDF15* expression increasing predominantly in the distal intestine and the**
39 **kidney. Metformin prevented weight gain in response to high fat diet in wild-**
40 **type mice but not in mice lacking GDF15 or its receptor GFRAL. In obese, high**
41 **fat-fed mice, the effects of metformin to reduce body weight were reversed by**
42 **a GFRAL antagonist antibody. Metformin had effects on both energy intake**
43 **and energy expenditure that required GDF15. Metformin retained its ability to**
44 **lower circulating glucose levels in the absence of GDF15 action. In summary,**
45 **metformin elevates circulating levels of GDF15, which are necessary for its**
46 **beneficial effects on energy balance and body weight, major contributors to its**
47 **action as a chemopreventive agent.**

48

49

50

51

52

53 Metformin has been used as a treatment for Type 2 diabetes since the 1950s.
54 Recent studies have shown that it can also prevent or delay the onset of Type 2
55 diabetes in people at high risk^{1,2}. At-risk individuals treated with metformin manifest
56 a reduction in body weight, glucose and insulin levels and enhanced insulin
57 sensitivity³. Although many mechanisms for the insulin sensitizing actions of
58 metformin have been proposed⁴, none would explain weight loss. The robustness
59 and persistence metformin-induced weight loss in participants in the Diabetes
60 Prevention Program (DPP) has drawn attention to the importance of this to the
61 chemopreventive effects of the drug⁵. A recent observational epidemiological study⁶
62 noted a strong association of metformin use with circulating levels of GDF15, a
63 peptide hormone produced by cells responding to stressors⁷. GDF15 acts through a
64 receptor complex solely expressed in the hindbrain, through which it suppress food
65 intake⁸⁻¹¹. We hypothesized that metformin's effects to lower body weight might
66 involve the elevation of circulating levels of GDF15.

67 **Human studies**

68 We first measured circulating GDF15 in a short term human study¹² and found that
69 after 2 weeks of metformin, there was a ~2.5-fold increase in mean circulating
70 GDF15 (**Fig. 1a**).

71 To determine if this increase was sustained, we measured circulating GDF15 levels
72 at 6, 12 and 18 months in all available participants in CAMERA¹³, a randomized
73 placebo-control trial of metformin in people without diabetes but with a history of
74 cardiovascular disease. In this study, metformin treated participants lost ~3.5% of
75 body weight with no significant change in weight in the placebo arm¹³. Metformin
76 treatment was associated with significantly ($p < 0.0001$) increased levels of

77 circulating GDF15 at all three time points (**Fig.1b** and **Extended Data Fig.1b,c,d,e**).
78 Furthermore, the change in serum GDF15 from baseline in metformin recipients was
79 significantly correlated ($r=-0.26$, $p=0.024$) with weight loss (**Extended Data Fig. 1a**).

80 The correlation of GDF15 increment with changes in body weight, while statistically
81 significant, was modest in size. While we consider it does contribute to weight loss in
82 some individuals taking metformin, we acknowledge is by no means necessary and
83 there are individuals with increases in GDF-15 that do not exhibit weight loss.
84 However, in the context of a long term human study with imperfect drug compliance
85 and intermittent sampling of GDF15 levels it is noteworthy that such an association
86 was seen at all. Further, there was no association of weight change with change in
87 GDF-15 in the placebo group ($r=-0.0374$, $p=0.740$, $n=81$).”

88 Murine studies

89 Following these findings in humans, we undertook a series of animal experiments to
90 determine the potential causal link between the changes in GDF-15 and weight
91 changes induced by metformin. We administered metformin to high fat diet fed mice
92 by oral gavage and measured serum GDF15. A single dose of 300 mg/kg of
93 metformin increased GDF15 levels for at least 8 hours (**Fig. 1c**). A higher dose of
94 metformin, 600 mg/kg, increased serum GDF15 levels 4-6 fold at 4 and 8-hours
95 post-dose, which were sustained over vehicle-treated mice for 24 hours. The effects
96 of metformin in chow-fed mice were less pronounced (**Extended Data Fig.2**)
97 suggesting an interaction between metformin and the high fat fed state.

98 To determine the extent to which metformin- induced increase in GDF15 affects
99 body weight, *Gdf15*^{+/+} and *Gdf15*^{-/-} mice were switched from chow to a high fat diet
100 and dosed with metformin for 11 days. High fat feeding induced similar weight gain

101 in both genotypes (**Fig. 2a**). Metformin completely prevented weight gain in *Gdf15*
102 ^{+/+} mice but *Gdf15*^{-/-} mice were insensitive to the weight-reducing effects of
103 metformin (**Fig.2a, Extended data Fig.3a**). Metformin significantly reduced
104 cumulative food intake in wild type mice but this effect was abolished in *Gdf15*^{-/-} mice
105 (**Fig. 2b**).

106

107 The identical protocol was applied to mice lacking GFRAL, the ligand-binding
108 component of the hindbrain-expressed GDF15 receptor complex. Consistent with
109 the results in mice lacking GDF15, metformin was unable to prevent weight gain in
110 *Gfral*^{-/-} mice (**Fig. 2c, Extended data Fig.3b**), despite similar levels of serum GDF15
111 (**Extended Data Fig. 4a,b**). In this experiment, the reduction in cumulative food
112 intake did not reach statistical significance (**Extended Data Fig. 4c**).

113 To investigate the contribution of GDF15/GFRAL signalling to sustained, metformin-
114 dependent weight regulation, we performed a 9-week study in which mice received
115 approximately 250-300 mg/kg/day of metformin incorporated into their high-fat diet.
116 The mice lost ~10% body weight after 1 month on this diet (**Fig. 2d**). At this time, an
117 anti-GFRAL antagonist antibody or IgG control was administered. Metformin-
118 consuming mice treated with anti-GFRAL regained ~12% body weight after 5 weeks,
119 while the weight loss seen in IgG control treated mice was maintained, reaching ~7%
120 below starting weight (**Fig. 2d**). The significant reduction in fat mass seen with
121 metformin treatment and control antibody was not seen in the anti-GFRAL group.
122 (**Extended Data Fig. 4d**). **The delivery of metformin in chow resulted in an initial**
123 **reduction in food intake in all metformin treated groups, presumably because of a**
124 **taste effect. This reduction in food intake will have affected metformin levels and is**

125 likely to have impacted GDF15 levels with potential to bias the results. However, it is
126 reassuring to note that any persistence of this would have worked against the
127 detection of a specific effect of GFRAL antagonism, which was clearly demonstrable.

128 We undertook indirect calorimetry in metformin- and placebo-treated mice treated
129 with anti-GFRAL antibody to establish whether there are additional effects on energy
130 expenditure. Data were analysed by ANCOVA with body weight as the co-variate.
131 Metformin treatment resulted in a significant increase in metabolic rate which was
132 blocked by antagonism of GFRAL (**Fig. 2e**). Thus under conditions where GDF15
133 levels are increased by metformin, body weight reduction is contributed to by both
134 reduced food intake and an inappropriately high energy expenditure.

135 GDF15 and glucose homeostasis

136 To examine the extent to which the insulin sensitising effects of metformin are
137 dependent on GDF15 we repeated the experiment described in **Fig.2a** (see
138 **Extended Data Fig. 5**), undertaking insulin tolerance testing in metformin and
139 vehicle-treated GDF15 null mice and their wild type littermates (**Fig. 3a**). Circulating
140 metformin levels achieved in both genotypes were identical (**Extended Data Fig. 5d**)
141 and consistent with the high end of the human therapeutic range ¹⁴. Metformin
142 significantly increased insulin sensitivity as assessed by the area under the plasma
143 glucose curve with no significant effect of genotype (**Fig. 3b**). Similarly, metformin
144 reduced fasting blood glucose and fasting insulin in a GDF15-independent manner
145 (**Fig. 3 c,d**).

146 We also undertook oral glucose tolerance testing of metformin treated mice given
147 either control IgG or anti-GFRAL antibody for 5 weeks (**Fig 3e,f, Extended Data**
148 **Fig. 6a** and see **Fig. 2d**). Although the effect of metformin glucose disposal at OGTT

149 as assessed by the area under the plasma glucose curve did not reach statistical
150 significance (2W ANOVA, $p=0.072$), there was a significant effect of metformin on
151 insulin, both fasting and AUC after glucose bolus, that was independent of antibody
152 **(Fig. 3 g,h,i,j)**.

153 As these mice were of different body weight at the time of assessment (**Fig. 2d** and
154 **Extended Data Fig. 3c**), we undertook further glucose tolerance testing in a cohort
155 of weight matched *Gdf15*^{+/+} and *Gdf15*^{-/-} mice that had been fed a high fat diet for 2
156 weeks before receiving a single dose of metformin (300mg/kg) (**Fig 3k,l** and
157 **Extended Data Fig. 6b-d**) In these mice there was a significant effect of metformin
158 upon glucose (AUC plasma glucose) that was independent of GDF15 (extended
159 Data Fig. 6 e).

160 Metformin's effect to lower fasting glucose and insulin and to improve glucose
161 tolerance appear not to require GDF15. Given the "a priori" expected effect of weight
162 loss on insulin sensitivity it is worthy of comment that the effect of GDF15 status on
163 insulin sensitivity as measured by ITT (**Fig 3b**) fell just short of statistical
164 significance. In the follow up of the DPP study in non-diabetic individuals, weight
165 loss after 5 years of metformin therapy was approximately 6.5% of baseline weight⁵ .
166 We therefore estimated the effect of a 6.5% weight loss on improvements in fasting
167 insulin over 5 years in the Ely Study, a prospective observational population-based
168 cohort study of men (n=465) and women (n=634) in the UK (mean age 52 years,
169 mean BMI 26 at baseline)¹⁵ , showing that this magnitude of weight loss was
170 associated with a reduction in fasting plasma insulin (mean $\pm 95\%$ CI) of -5.74 (-
171 9.03, -2.45) pmol/l in women and -8.78 (-16.24, -1.33) in men. We conclude that
172 while there are GDF15-independent effects of metformin on circulating levels of

173 glucose and insulin, it is likely that the GDF15 dependent weight loss will make a
174 contribution to enhancing insulin sensitivity.

175

176 **Source of GDF15 production**

177 We examined GDF15 gene expression in a tissue panel obtained from mice fed a
178 high fat diet (for 4 weeks) and sacrificed 6 hours after a single gavage dose of
179 metformin (600mg/kg). Circulating concentrations of GDF15 increased ~4-fold
180 compared to vehicle treated mice (**Extended Data Fig. 6f**). *Gdf15* mRNA was
181 significantly increased by metformin in small intestine, colon and kidney. (**Fig. 4a**). In
182 situ hybridisation studies demonstrated strong *Gdf15* expression in crypt enterocytes
183 in the colon and small intestine and in periglomerular renal tubular cells (**Fig. 4b**,
184 **Extended Data Fig. 7a, b**). We confirmed these sites of tissue expression in HFD
185 fed mice (those used in **Fig 2a**), treated with metformin for 11 days (**Extended Data**
186 **Fig. 8**).

187 Further, in human (**Fig. 4c**) and murine (**Fig. 4d**) intestinal-derived organoids grown
188 in 2D transwells and treated with metformin, we saw a significant induction of mRNA
189 expression and GDF15 protein secretion.

190 Given the proposed importance of the liver for metformin's metabolic action it was
191 notable that the dominant GDF15 expression signal was not from the liver (**Fig. 4a**,
192 **Extended Data Fig. 7a, Extended Data Fig. 8**). To test whether hepatocytes are
193 capable of responding to biguanide drugs with an increase in GDF15 we incubated
194 freshly isolated murine hepatocytes (**Extended Data Fig. 9a**) and stem-cell derived
195 human hepatocytes (**Extended Data Fig. 9b**) with metformin and found a clear
196 induction of GDF15 expression. Additionally, acute administration of the more cell

197 penetrant biguanide drug phenformin to mice increased circulating GDF15 levels
198 (**Extended Data Fig. 9c**) and markedly increased *Gdf15* mRNA expression in
199 hepatocytes (**Extended Data Fig. 9d,e**). We conclude that biguanides can induce
200 GDF15 expression in many cell types, but at least when given orally to mice, GDF15
201 mRNA is most strikingly induced in the distal small intestine, colon and kidney.

202 GDF15 expression has been reported to be a downstream target of the cellular
203 integrated stress response (ISR) pathway¹⁶⁻¹⁸. *Gdf15* mRNA levels were increased in
204 kidney and colon 24 h after a single oral dose of metformin and these changes
205 correlated positively with the fold elevation of CHOP mRNA (**Extended Data Fig.**
206 **10a,b**). As phenformin has broader cell permeability than metformin¹⁹ we used it to
207 explore the effects of biguanides on the ISR and its relationship to GDF15
208 expression in cells. In murine embryonic fibroblasts (MEFs), which do not express
209 the organic cation transporters needed for the uptake of metformin, phenformin (but
210 not metformin) increased EIF2 α phosphorylation, ATF4 and CHOP expression,
211 (**Extended Data Fig. 10c**) and GDF15 mRNA (**Extended Data Fig. 10d**), though the
212 changes in EIF2a phosphorylation and ATF4 and CHOP expression were modest
213 compared with those induced by tunicamycin despite similar levels of GDF15 mRNA
214 induction. Both genetic deletion of ATF4 and siRNA-mediated knockdown of CHOP
215 significantly reduced phenformin-mediated induction of GDF15 mRNA expression
216 (**Extended Data Fig. 10e,f**). In addition, phenformin induction of GDF15 was
217 markedly reduced by co-treatment with the EIF2 α inhibitor, ISRIB but, notably, not by
218 the PERK inhibitor, GSK2606414 (**Extended Data Fig. 10g**). Further, GDF15
219 secretion in response to metformin in murine duodenal organoids was also
220 significantly reduced by co-treatment with ISRIB (**Extended Data Fig. 10h**).
221 However, gut organoids derived from CHOP null mice are still able to increase

222 GDF15 secretion in response to metformin (**Extended Data Fig. 10i**) indicating the
223 existence of CHOP-independent pathways under some circumstances. The data
224 suggest that the effects of biguanides on GDF15 expression are at least partly
225 dependent on the ISR pathway but are independent of PERK. However, the relative
226 importance of components of the ISR pathway may vary depending on specific cell
227 type, dose and agent used.

228 Our observations represent a significant advance in our understanding of the action
229 of metformin, one of the world's most frequently prescribed drugs. Metformin
230 increases circulating GLP1 levels²⁰⁻²² , but its metabolic effects in mice are
231 unimpaired in mice lacking the GLP-1 receptor ²³. Metformin alters the intestinal
232 microbiome^{24,25} but it is challenging to firmly establish a causal relationship to the
233 beneficial effects of the drug ²⁶.

234 In the work presented herein, we describe a body of data from humans, cells,
235 organoids and mice that securely establish a major role for GDF15 in the mediation
236 of metformin's beneficial effects on energy balance. While these effects likely
237 contribute to metformin's role as an insulin sensitizer, metformin continues to have
238 effects to lower glucose and insulin in the absence of GDF15.

239

240 While there have been many mechanisms suggested for the glucoregulatory
241 mechanisms of metformin²⁷ there has been less attention paid to its effects on
242 weight. Our discoveries relating to metformin's effects via GDF15 provide a
243 compelling explanation for this important aspect of metformin action.

244 It is notable that the lower small intestine and colon are a major site of metformin
245 induced GDF15 expression. A body of work is emerging which strongly implicates
246 the intestine as a major site of metformin action. Metformin increased glucose uptake

247 into colonic epithelium from the circulation²⁸ and a gut-restricted formulation of
248 metformin had greater glucose lowering efficacy than systemically absorbed
249 formulations²⁹. Our finding that the intestine is a major site of metformin-induced
250 GDF15 expression provides a further mechanism through which metformin's action
251 on the intestinal epithelium may mediate some of its benefits.

252 **References.**

- 253 1 Knowler, W. C. *et al.* Reduction in the incidence of type 2 diabetes with lifestyle intervention
254 or metformin. *N Engl J Med* **346**, 393-403, doi:10.1056/NEJMoa012512 (2002).
- 255 2 Ramachandran, A. *et al.* The Indian Diabetes Prevention Programme shows that lifestyle
256 modification and metformin prevent type 2 diabetes in Asian Indian subjects with impaired
257 glucose tolerance (IDPP-1). *Diabetologia* **49**, 289-297, doi:10.1007/s00125-005-0097-z
258 (2006).
- 259 3 Lachin, J. M. *et al.* Factors associated with diabetes onset during metformin versus placebo
260 therapy in the diabetes prevention program. *Diabetes* **56**, 1153-1159, doi:10.2337/db06-
261 0918 (2007).
- 262 4 Rena, G., Hardie, D. G. & Pearson, E. R. The mechanisms of action of metformin.
263 *Diabetologia* **60**, 1577-1585, doi:10.1007/s00125-017-4342-z (2017).
- 264 5 Apolzan, J. W. *et al.* Long-Term Weight Loss With Metformin or Lifestyle Intervention in the
265 Diabetes Prevention Program Outcomes Study. *Ann Intern Med*, doi:10.7326/M18-1605
266 (2019).
- 267 6 Gerstein, H. C. *et al.* Growth Differentiation Factor 15 as a Novel Biomarker for Metformin.
268 *Diabetes Care* **40**, 280-283, doi:10.2337/dc16-1682 (2017).
- 269 7 Tsai, V. W. W., Husaini, Y., Sainsbury, A., Brown, D. A. & Breit, S. N. The MIC-1/GDF15-GFRAL
270 Pathway in Energy Homeostasis: Implications for Obesity, Cachexia, and Other Associated
271 Diseases. *Cell Metab* **28**, 353-368, doi:10.1016/j.cmet.2018.07.018 (2018).
- 272 8 Mullican, S. E. *et al.* GFRAL is the receptor for GDF15 and the ligand promotes weight loss in
273 mice and nonhuman primates. *Nat Med* **23**, 1150-1157, doi:10.1038/nm.4392 (2017).
- 274 9 Emmerson, P. J. *et al.* The metabolic effects of GDF15 are mediated by the orphan receptor
275 GFRAL. *Nat Med* **23**, 1215-1219, doi:10.1038/nm.4393 (2017).
- 276 10 Yang, L. *et al.* GFRAL is the receptor for GDF15 and is required for the anti-obesity effects of
277 the ligand. *Nat Med* **23**, 1158-1166, doi:10.1038/nm.4394 (2017).
- 278 11 Hsu, J. Y. *et al.* Non-homeostatic body weight regulation through a brainstem-restricted
279 receptor for GDF15. *Nature* **550**, 255-259, doi:10.1038/nature24042 (2017).
- 280 12 Konopka, A. R. *et al.* Hyperglucagonemia Mitigates the Effect of Metformin on Glucose
281 Production in Prediabetes. *Cell Rep* **15**, 1394-1400, doi:10.1016/j.celrep.2016.04.024 (2016).
- 282 13 Preiss, D. *et al.* Metformin for non-diabetic patients with coronary heart disease (the
283 CAMERA study): a randomised controlled trial. *Lancet Diabetes Endocrinol* **2**, 116-124,
284 doi:10.1016/S2213-8587(13)70152-9 (2014).
- 285 14 McCreight, L. J. *et al.* Pharmacokinetics of metformin in patients with gastrointestinal
286 intolerance. *Diabetes Obes Metab* **20**, 1593-1601, doi:10.1111/dom.13264 (2018).
- 287 15 Forouhi, N. G., Luan, J., Hennings, S. & Wareham, N. J. Incidence of Type 2 diabetes in
288 England and its association with baseline impaired fasting glucose: the Ely study 1990-2000.
289 *Diabet Med* **24**, 200-207, doi:10.1111/j.1464-5491.2007.02068.x (2007).
- 290 16 Chung, H. K. *et al.* Growth differentiation factor 15 is a myomitokine governing systemic
291 energy homeostasis. *J Cell Biol* **216**, 149-165, doi:10.1083/jcb.201607110 (2017).

292 17 Li, D., Zhang, H. & Zhong, Y. Hepatic GDF15 is regulated by CHOP of the unfolded protein
293 response and alleviates NAFLD progression in obese mice. *Biochem Biophys Res Commun*
294 **498**, 388-394, doi:10.1016/j.bbrc.2017.08.096 (2018).

295 18 Patel, S. *et al.* GDF15 Provides an Endocrine Signal of Nutritional Stress in Mice and Humans.
296 *Cell Metab* **29**, 707-718 e708, doi:10.1016/j.cmet.2018.12.016 (2019).

297 19 Shu, Y. *et al.* Effect of genetic variation in the organic cation transporter 1 (OCT1) on
298 metformin action. *J Clin Invest* **117**, 1422-1431, doi:10.1172/JCI30558 (2007).

299 20 DeFronzo, R. A. *et al.* Once-daily delayed-release metformin lowers plasma glucose and
300 enhances fasting and postprandial GLP-1 and PYY: results from two randomised trials.
301 *Diabetologia* **59**, 1645-1654, doi:10.1007/s00125-016-3992-6 (2016).

302 21 Preiss, D. *et al.* Sustained influence of metformin therapy on circulating glucagon-like
303 peptide-1 levels in individuals with and without type 2 diabetes. *Diabetes Obes Metab* **19**,
304 356-363, doi:10.1111/dom.12826 (2017).

305 22 Bahne, E. *et al.* Metformin-induced glucagon-like peptide-1 secretion contributes to the
306 actions of metformin in type 2 diabetes. *JCI Insight* **3**, doi:10.1172/jci.insight.93936 (2018).

307 23 Maida, A., Lamont, B. J., Cao, X. & Drucker, D. J. Metformin regulates the incretin receptor
308 axis via a pathway dependent on peroxisome proliferator-activated receptor-alpha in mice.
309 *Diabetologia* **54**, 339-349, doi:10.1007/s00125-010-1937-z (2011).

310 24 de la Cuesta-Zuluaga, J. *et al.* Metformin Is Associated With Higher Relative Abundance of
311 Mucin-Degrading Akkermansia muciniphila and Several Short-Chain Fatty Acid-Producing
312 Microbiota in the Gut. *Diabetes Care* **40**, 54-62, doi:10.2337/dc16-1324 (2017).

313 25 Shin, N. R. *et al.* An increase in the Akkermansia spp. population induced by metformin
314 treatment improves glucose homeostasis in diet-induced obese mice. *Gut* **63**, 727-735,
315 doi:10.1136/gutjnl-2012-303839 (2014).

316 26 Forslund, K. *et al.* Disentangling type 2 diabetes and metformin treatment signatures in the
317 human gut microbiota. *Nature* **528**, 262-266, doi:10.1038/nature15766 (2015).

318 27 Foretz, M., Guigas, B. & Viollet, B. Understanding the gluco regulatory mechanisms of
319 metformin in type 2 diabetes mellitus. *Nat Rev Endocrinol* **15**, 569-589, doi:10.1038/s41574-
320 019-0242-2 (2019).

321 28 Massollo, M. *et al.* Metformin temporal and localized effects on gut glucose metabolism
322 assessed using 18F-FDG PET in mice. *J Nucl Med* **54**, 259-266,
323 doi:10.2967/jnumed.112.106666 (2013).

324 29 Buse, J. B. *et al.* The Primary Glucose-Lowering Effect of Metformin Resides in the Gut, Not
325 the Circulation: Results From Short-term Pharmacokinetic and 12-Week Dose-Ranging
326 Studies. *Diabetes Care* **39**, 198-205, doi:10.2337/dc15-0488 (2016).

327

328

329

330

331 **Figure Legend**

332 **Figure 1. Effect of Metformin on circulating GDF15 levels in humans and mice.**

333 **a**, Paired serum GDF15 concentration in 9 human subjects after 2 weeks of either
334 placebo or metformin, P (95% confidence interval) by 2-tailed t-test.

335 **b**, Plasma GDF15 concentration (mean± SEM) in overweight or obese non-diabetic
336 participants with known cardiovascular disease randomised to metformin or placebo
337 in CAMERA, using a mixed linear model. Subject numbers: placebo vs metformin,

338 respectively, at time points: baseline, n=85 vs n=86; 6 months, n=81 vs n= 71;12
339 months, n=77 vs n=68; 18 months, n=83 vs n=74. Comparing metformin vs placebo
340 groups, two-sided p=0.311 at baseline, and p<0.0001 at 6,12 and 18 months
341 individually.

342 **c**, Serum GDF15 levels (mean± SEM) in obese mice measured 2, 4, 8 or 24 hours
343 after a single oral dose of 300 mg/kg or 600 mg/kg metformin, n=7/group, P by 2-way
344 ANOVA with Tukey's correction for multiple comparisons.

345

346 **Figure 2. GDF15/GFRAL signalling is required for the weight loss effects of**
347 **metformin on a high fat diet.**

348 **a**, Percentage change in body weight of Gdf15+/+ and Gdf15-/- mice on a high-fat
349 diet treated with metformin (300mg/kg/day) for 11 days, mean ± SEM, n=6/group
350 except Gdf15+/+ vehicle n=7, P by 2-way ANOVA with Tukey's correction for
351 multiple comparisons.

352 **b**, Cumulative food intake of mice as Figure 2a, P by 2-way ANOVA with Tukey's
353 correction for multiple comparisons.

354 **c**, Percentage change in body weight of Gfral+/+ and Gfral-/- mice on a high-fat diet
355 treated with metformin (300mg/kg/day) for 11 days, mean ± SEM, n=6/groups, P by
356 2-way ANOVA with Tukey's correction for multiple comparisons.

357 **d**, Percentage change in body weight of metformin-treated obese mice dosed with
358 an anti-GFRAL antagonist antibody, weekly for 5 weeks (yellow), starting 4 weeks
359 after initial metformin exposure (grey), mean ± SEM, n=7 Vehicle + control IgG and
360 Metformin + anti -GFRAL, n=8 other groups, P by 2-way ANOVA with Tukey's
361 correction for multiple comparisons. "calo" = period in which energy expenditure
362 measured (see Figure 2e), Arrow and "GTT"- timing of oral glucose tolerance test
363 (see Figure 3e-h).

364 **e**, ANCOVA analysis of energy expenditure against body weight of mice treated as in
365 Figure 2d, n=6 mice/group. Data are individual mice and P for metformin calculated
366 using ANCOVA with body weight as a covariate and treatment as a fixed factor.

367

368 **Figure 3. Effects of metformin on glucose homeostasis.**

369 **a**, Insulin tolerance test (ITT) (insulin=0.5 U/kg) after 11 days of metformin treatment
370 (300mg/kg) to high fat fed Gdf15 +/+ and Gdf15 -/- mice, glucose levels are mean ±
371 SEM, n=6/group, except Gdf15 -/- vehicle= 7, Gdf15+/+ vehicle= 5.

372 **b**, Area under curve (AUC) analysis of glucose over time in Figure 3a, mean ± SEM,
373 P by 2-way ANOVA , interaction of genotype and metformin p= 0.037.

374 **c**, Fasting glucose (time 0) of ITT in Figure 3a, mean ± SEM, P by 2-way ANOVA,
375 effect of genotype p= 0.144, interaction of genotype and metformin p= 0.988.

376 **d**, Fasting insulin (time 0) of ITT in Figure 3a, mean \pm SEM, P by 2-way ANOVA,
377 effect of genotype $p= 0.131$, interaction of genotype and metformin $p 0.056$.

378 **e, f**, Glucose over time after oral glucose tolerance test (GTT) in metformin treated
379 obese mice given either IgG (e) or anti –GFRAL (f) once weekly for 5 weeks (as
380 Figure 2d). AUC analysis by 2-way ANOVA, effect of antibody $p= 0.031$, effect of
381 metformin $p= 0.072$, interaction of antibody and metformin $p 0.91$.

382 **g, h**, Insulin (mean \pm SEM) over time after GTT in mice as Figure 3e and f.

383 **i**, Fasting insulin (time 0) of GTT in mice as Figure 3e and f, mean \pm SEM, P by 2-
384 way ANOVA, effect of antibody $p= 0.544$, interaction of genotype and metformin p
385 0.691 .

386 **j**, AUC analysis of insulin over time in Figure 3g and h, mean \pm SEM, P by 2 -way
387 ANOVA, effect of antibody $p= 0.197$, interaction of genotype and metformin $p 0.607$.

388 **k, l**, Glucose (mean \pm SEM) over time after intraperitoneal GTT in high fat fed mice
389 given single dose of oral metformin (300mg/kg) 6 hrs before GTT, $n=8$ /group.

390

391 **Figure 4. Metformin increases GDF15 expression in the enterocytes of distal**
392 **intestine and the renal tubular epithelial cells.**

393 **a**, Gdf15 mRNA expression (normalised to expression levels of ActB) in tissues from
394 high-fat fed wild type mice 6 hrs after single dose of oral metformin (600mg/kg),
395 mean \pm SEM, $n=7$ /group, P value (95% confidence interval) by two tailed t-test.

396 **b**, In situ hybridization for Gdf15 mRNA (red spots) $n= 7$ per group. Representative
397 images from the mouse with circulating GDF15 level closest to group median, either
398 vehicle-treated (panel 1a,1b,1c, blue box) or metformin-treated (panels 2a, 2b, 2c,
399 red box). Mice from groups described in Figure 4a.

400 **c**, Gdf15 mRNA expression (left panel) and GDF15 protein in supernatant (right
401 panel) of human derived 2D monolayer rectal organoids treated with metformin.
402 Each colour represents independent experiments ($n= 4$), mean \pm SD, P value (95%
403 confidence interval) by two-tailed t-test.

404 **d**, GDF15 protein in supernatants of mouse-derived 2D monolayer duodenal (left
405 panel) and ileal (right panel) organoids treated with metformin. Each colour
406 represents independent experiment (duodenal $n= 5$, ileal $n=3$),mean \pm SD, P value
407 (95% confidence interval) by two-tailed t-test.

408

409

410

411

412 **Methods.**

413 **Human Studies.**

414 We analysed samples from 9 participants from a study with a placebo-controlled,
415 double-blind crossover design (previously described in¹²). In brief, placebo or
416 metformin (week 1, 500mg twice daily; week, 2 1000mg twice daily) were
417 administered following a six week period of washout. Samples were collected in the
418 morning after overnight fasting. The study was approved by the Mayo Clinic
419 Institutional Review Board and all participants provided written, informed consent
420 (NCT01956929).

421 CAMERA was a randomized, double-blinded, placebo-controlled trial designed to
422 investigate the effect of metformin on surrogate markers of cardiovascular disease in
423 patients without diabetes, aged 35 to 75, with established coronary heart disease
424 and a large waist circumference (≥ 94 cm in men, ≥ 80 cm in women)
425 (NCT00723307). This single-centre trial enrolled 173 adults who were followed up for
426 18 months each. A detailed description of the trial and its results has been published
427 previously¹³. In brief, participants were randomized 1:1 to 850mg metformin or
428 matched placebo twice daily with meals. Participants attended six monthly visits after
429 overnight fasts and before taking their morning dose of metformin. Blood samples
430 collected during the trial were centrifuged at 4 degrees Celsius soon after sampling,
431 separated and stored at -80°C

432 All participants provided written informed consent. The study was approved by the
433 Medicines and Healthcare Products Regulatory Agency and West Glasgow
434 Research Ethics Committee, and done in accordance with the principles of the
435 Declaration of Helsinki and good clinical practice guidelines.

436 Serum GDF15 assays were completed by the Cambridge Biochemical Assay
437 Laboratory, University of Cambridge. Measurements were undertaken with
438 antibodies & standards from R&D Systems (R&D Systems Europe, Abingdon UK)
439 using a microtiter plate-based two-site electrochemiluminescence immunoassay
440 using the MesoScale Discovery assay platform (MSD, Rockville, Maryland, USA).

441 **Mouse Studies.**

442 Studies were carried out in two sites; NGM Biopharmaceuticals, California, USA and
443 University of Cambridge, UK.

444 At NGM, all experiments were conducted with NGM IACUC approved protocols and
445 all relevant ethical regulations were complied with throughout the course of the
446 studies, including efforts to reduce the number of animals used. Experimental
447 animals were kept under controlled light (12hour light and 12hour dark cycle, dark
448 6:30 pm - 6:30 am), temperature ($22 \pm 3^{\circ}\text{C}$) and humidity ($50\% \pm 20\%$) conditions.
449 They were fed ad libitum on 2018 Teklad Global 18% Protein Rodent Diet containing
450 24 kcal% fat, 18 kcal% protein and 58 kcal% carbohydrate, or on high fat rodent diet
451 containing 60 kcal% fat, 20 kcal% protein and 20 kcal% carbohydrates from
452 Research Diets D12492i,(New Brunswick NJ 089901 USA) herein referred to as
453 "60%HFD".

454 In Cambridge, all mouse studies were performed in accordance with UK Home
455 Office Legislation regulated under the Animals (Scientific Procedures) Act 1986
456 Amendment, Regulations 2012, following ethical review by the University of
457 Cambridge Animal Welfare and Ethical Review Body (AWERB). They were
458 maintained in a 12-hour light/12-hour dark cycle (lights on 0700–1900),
459 temperature-controlled (22°C) facility, with ad libitum access to food (RM3(E))

460 Expanded chow, Special Diets Services, UK) and water. Any mice bought from an
461 outside supplier were acclimatised in a holding room for at least one week prior to
462 study. During study periods they were fed ad libitum high fat diet, either D12451i (45
463 kcal% fat, 20 kcal% protein and 35 kcal% carbohydrates, herein referred to as
464 “45%HFD”) or D12492i (Research Diets, as above) as highlighted in individual
465 study.

466 Sample sizes were determined on the basis of homogeneity and consistency of
467 characteristics in the selected models and were sufficient to detect statistically
468 significant differences in body weight, food intake and serum parameters between
469 groups. Experiments were performed with animals of a single gender in each study.
470 Animals were randomized into the treatment groups based on body weight such that
471 the mean body weights of each group were as close to each other as possible, but
472 without using excess number of animals. No samples or animals were excluded from
473 analyses. Researchers were not blinded to group allocations.

474 **Mouse study 1. Acute two- dose metformin study in high fat diet fed mice.**

475 Male C57Bl6/J mice fed 60% HFD for 17 weeks were studied aged 23 weeks (body
476 weight, mean±SEM, 45.6±0.8g). Metformin (Sigma-Aldrich # 1396309) was
477 reconstituted in water at 30 mg/ml for oral gavage and given in early part of light
478 cycle. Terminal blood was collected by cardiac puncture into EDTA- coated tubes.
479 GDF15 levels were measured using Mouse/Rat GDF15 Quantikine ELISA Kit (Cat#:
480 MGD-150, R&D Systems, Minneapolis, MN) according to the manufacturers'
481 instructions. RNA was isolated from tissues using the Qiagen RNeasy Kit. RNA was
482 quantified and 500ng was used for cDNA synthesis (SuperScript VILO 11754050
483 ThermoFisher) followed by qPCR. All Taqman probes were purchased from Applied

484 Biosystems. All genes are expressed relative to 18s control probe and were run in
485 triplicate.

486

487 **Mouse study 2. Acute metformin study in chow fed animals.**

488 **2.i) ad libitum group.**

489 Male C57BL6/J mice (Charles River, Margate, UK) were studied at 11 weeks old.
490 500mg of metformin was dissolved in 20 mls of water to make a working stock of
491 25mg/ml. 1 hr after onset of light cycle mice received a single dose by oral gavage
492 of either metformin at 300mg/kg dose (Sigma, PHR1084-500MG) or matched
493 volume of vehicle (water). Weight (mean \pm SEM) of control and treatment groups
494 were 27.2 \pm 0.3 vs 26.7 \pm 0.2 g, respectively on day of study. After gavage mice
495 were returned to an individual cage and were sacrificed at relevant time point by
496 terminal anaesthesia (Euthatal by Intraperitoneal injection). Blood was collected
497 into Sarstedt Serum Gel 1.1ml Micro Tube, left for 30mins at room temperature,
498 spun for 5mins at 10k at 40C before being frozen and stored at -80oC until assayed.
499 Mouse GDF15 levels were measured using a Mouse GDF15 DuoSet ELISA (R&D
500 Systems) which had been modified to run as an electrochemiluminescence assay on
501 the Meso Scale Discovery assay platform.

502 **2.ii) fasted group.**

503 Mice, conditions and methods as in (2.i) except male mice studied at 9 weeks old
504 and that 12 hr prior to administration of metformin mice and bedding were
505 transferred to new cages with no food in hopper. Weight (mean \pm SEM) after fasting
506 and on day of gavage were 22.3 \pm 0.5 g and 23.2 \pm 0.7g for control and treatment
507 groups, respectively.

508 **Mouse study 3. Metformin to high fat diet fed *Gdf15*^{-/-} mice and wild type**
509 **controls.**

510 C57BL/6N-Gdf15tm1a(KOMP)Wtsi/H mice (herein referred to as “Gdf15^{-/-} mice“)
511 were obtained from the MRC Harwell Institute which distributes these mice on behalf
512 of the European Mouse Mutant Archive (www.infrafrontier.eu). The MRC Harwell
513 Institute is also a member of the International Mouse Phenotyping Consortium
514 (IMPC) and has received funding from the MRC for generating and/or phenotyping
515 the C57BL/6N-Gdf15tm1a(KOMP)Wtsi/H mice. The research reported in this
516 publication is solely the responsibility of the authors and does not necessarily
517 represent the official views of the Medical Research Council. Associated primary
518 phenotypic information may be found at www.mousephenotype.org. Details of the
519 alleles have been published³⁰⁻³².

520 Experimental cohorts of male *Gdf15*^{-/-} and wild type mice were generated by het x
521 het breeding pairs. Mice were aged between 4.5 and 6.5 months. One week prior to
522 study start mice were single housed and 3 days prior to first dose of metformin
523 treatment, mice were transferred from standard chow to 60% high fat diet. On day of
524 first gavage body weight of study groups (mean±SEM) were 38.2±1.0g vs 38.8±0.6g
525 for wild type vehicle and metformin treatment respectively, and 37.9±0.8g vs
526 37.0±1.4g for *Gdf15*^{-/-} vehicle and metformin treatment respectively. Each mouse
527 received a daily gavage of either vehicle or metformin for 11 days, and their body
528 weight and food intake measured daily in the early part of the light cycle. One data
529 point of 25 food intake points collected on day11 of study was lost due to technical
530 error (mouse; *Gdf15*^{+/+} metformin). On day 11 mice were sacrificed by terminal
531 anaesthesia 4 hours post gavage, blood was obtained as in study 2. Tissues were
532 fresh frozen on dry ice and kept at -80⁰C until day of RNA extraction.

533

534 **Mouse study 4. Metformin to high fat diet fed *Gfrol*^{-/-} mice.**

535 *Gfrol*^{-/-} mice were purchased from Taconic (#TF3754) on a mixed 129/SvEv-C57BL/6
536 background and backcrossed for 10 generations to >99% C57BL/6 background at
537 NGM's animal facility. Experimental cohorts were generated by het X het breeding
538 pairs. Study design as Study 3, except terminal blood was collected into EDTA-
539 coated tubes.

540 **Mouse study 5. Anti GFRAL antibody to metformin treated high fat diet fed**
541 **mice.**

542 **Anti-GFRAL antibody generation.** Anti-GFRAL monoclonal antibodies were
543 generated by immunizing C57Bl/6 mice with recombinant purified GFRAL ECD-hFc
544 fusion protein, which was purified via sequential protein-A affinity and size exclusion
545 chromatography (SEC) techniques using MabSelect SuRe and Superdex 200
546 purification media respectively (GE Healthcare), as described in patent number
547 US10174119B2, <https://patents.google.com/patent/US10174119B2/en>. An in-house
548 pTT5 hlgK hlgG1 expression vector was engineered to include the DEVDG
549 (caspase-3) proteolytic site N-terminal to the Fc domain. The heavy chains of anti-
550 GFRAL mAbs were subcloned via EcoR1/HindIII sites of in-house engineered pTT5
551 hlgK hlgG1 caspase-cleavable vector. Light chains of anti-GFRAL mAbs were also
552 subcloned within the EcoR1/HindIII sites in the pTT5 hlgK hKappa vector. The
553 antibody were transiently expressed in Expi293 cells (Thermo Fisher Scientific)
554 transfected with the pTT5 expression vector, and purified from conditioned media by
555 sequential protein-A affinity and size-exclusion chromatographic (SEC) methods
556 using MabSelect SuRe and Superdex 200 purification media respectively (GE

557 Healthcare). All purified antibody material was verified endotoxin-free and formulated
558 in PBS for in vitro and in vivo studies. Characterization of anti-GFRAL functional
559 blocking antibodies was carried out using a cell-based RET/GFRAL luciferase gene
560 reporter assays, in vitro binding studies (ELISA and Biacore) and in vivo studies, as
561 described in patent number; US10174119B2,
562 <https://patents.google.com/patent/US10174119B2/en>).

563 In all studies with anti-GFRAL, purified recombinant non-targeting IgG on the same
564 antibody framework was used as control. Metformin was mixed with food paste
565 made from the 60 kcal% fat diet (Research diet# D12492) using a food blender at a
566 concentration to achieve an approximate consumption of 300mg/kg metformin per
567 day per mouse. Male animals were single housed throughout and at start of study
568 period body weight (mean \pm SEM) was 43.7 \pm 1.4g, 42.3 \pm 1.4g, 41.9 \pm 1.1g, 43.3 \pm 1.3g,
569 veh + control IgG, veh +anti-GFRAL, metformin + control IgG, Metformin + anti-
570 GFRAL, respectively. Recombinant antibodies were administered by subcutaneous
571 injection in the early part of the light cycle. Body composition (lean and fat mass)
572 was analyzed by ECHO MRI M113 mouse system (Echo Medical Systems). The
573 metabolic parameters oxygen consumption (VO₂) and carbon dioxide production
574 (VCO₂) were measured by an indirect calorimetry system (LabMaster TSE System,
575 Germany) in open circuit sealed chambers. Measurements were performed for the
576 dark (from 6pm to 6am) or light (from 6am to 6pm) period under ad libitum feeding
577 conditions. Mice were placed in individual metabolic cages and allowed to acclimate
578 for a period of 24 hours prior to data collection in every 30 minutes.

579 Finally, mice underwent a glucose tolerance test. Mice were fasted for 6 hours
580 (7am-1pm) in a clean cage. Blood samples (~30 ul) were collected as baseline prior
581 to oral glucose tolerance test. Mice were orally gavaged with 1 g/kg of 20% glucose

582 solution with a dosing volume of 5 mL/kg. Blood samples were then collected
583 through tail nick into K2EDTA-coated tubes (SARSTEDT Microvette; REF
584 20.1278.100) at 15, 30, 60 and 120 minutes post glucose challenge. Blood samples
585 were centrifuged at 4 °C and the separated plasma are stored at -20 °C until used
586 for plasma glucose and insulin assays. Glucose assay reagents obtained from
587 Wako, Cat# 439-90901, and the insulin ELISA kit obtained from ALPCO, Cat# 80-
588 INSMSU-E01.

589

590 **Mouse study 6. Insulin tolerance test after metformin treatment to high fat diet**
591 **fed *Gdf15*^{-/-} and wild type controls.**

592 Mice generation and protocol as Study 3, except aged 4 to 6 months. On day of first
593 gavage body weights (mean±SEM) of study groups were 35.1±1.2g; 35.05±1.2g for
594 wild type Vehicle and Metformin treatment respectively, and 35.08±1.02g;
595 35.02±1.47g for *Gdf15*^{-/-} Vehicle and Metformin treatment respectively. On day 11,
596 after final dose of metformin mice were fasted for 4 hours. Baseline venous blood
597 sample was collected into heparinised capillary tube for insulin measurement and
598 blood glucose was measured using approximately 2 µl blood drops using a
599 glucometer (AlphaTrak2; Abbot Laboratories) and glucose strips (AlphaTrak2 test 2
600 strips, Abbot Laboratories, Zoetis) .Mice were given intraperitoneal injection of insulin
601 (0.5U/kg mouse, Actrapid, NovoNordisk Ltd) and serial mouse glucose levels
602 measured at time points indicated. Mice were sacrificed by terminal anaesthesia as
603 in Study 2. Mouse insulin was measured using a 2-plex Mouse Metabolic
604 immunoassay kit from Meso Scale Discovery Kit (Rockville, MD, USA), performed
605 according to the manufacturer's instructions and using calibrators provided by MSD.

606 Serum metformin levels were quantified using a stable isotope dilution LC-MS/MS
607 method described previously³³.

608 **Mouse study 7. Glucose tolerance test after single dose metformin treatment**
609 **to high fat diet fed Gdf15^{-/-} and wild type controls.**

610 Mice generation as Study 3, except female mice aged 3.5 to 5.5 months. 2 groups of
611 mice (*Gdf15*^{+/+} and *Gdf15*^{-/-} littermates, body weight (mean±S.E.M), 24.1 ±1.4g vs
612 24.3±1.3g , respectively) were fed 60% HFD for 2 weeks. Each genotype was then
613 further split into vehicle or metformin (300mg/kg) treatment group, given a single
614 gavage dose at 8am and fasted for 6 hrs. At time of GTT, body weights
615 (mean±S.E.M) of study groups were 26.4.1±1.5g; 26.5±1.0g for wild type Vehicle
616 and Metformin treatment respectively, and 25.6±1.2g; 27.1±1.3g for *Gdf15*^{-/-}
617 Vehicle and Metformin treatment respectively (1 way ANOVA, p=0.8722). Baseline
618 testing as mouse study 6. Mice then received a single dose of 20% glucose via
619 intraperitoneal route (2mg/g dose) with serial measurement of glucose levels
620 measured at time points indicated. Sacrifice and insulin analysis as mouse study 6.

621

622 **Mouse study 8. Acute single high dose metformin study in high fat diet fed**
623 **wild type mice.**

624 Male C57BL6/J mice (Charles River, Margate, UK) aged 14 weeks were switched
625 from standard chow to 45 %HFD fat (D12451i) for 1 week then 60%HFD (D12492i,
626 for 3 weeks). At time of study (18 weeks old) body weights (mean ±SEM) were 40.4±
627 1.2g vs 41.1±1.3g, vehicle vs metformin group, respectively. 500mg of metformin
628 (Sigma, PHR1084-500MG) was dissolved in 8.35 mls of water to make a working
629 stock of 60mg/ml. Mice received a single dose by oral gavage of either 600mg/kg

630 metformin or matched volume of vehicle (water). They were returned to ad lib 60 %
631 fat diet and 6 hrs later blood was collected as study 2. Tissue samples for RNA
632 analysis were collected into Lysing Matrix D homogenisation tube (MP Biomedicals)
633 on dry ice and stored at -80°C until processed. Intestine between pylorus of stomach
634 and caecum was laid out into 3 equal parts, with tissue taken from mid-point of each
635 third labelled as “proximal”, “ middle” and “ distal” (adapted from ³⁴). Colon section
636 was from mid-point between caecum and anus. Tissue for in-situ hybridisation were
637 dissected and placed into 10% formalin/PBS for 24hr at room temp, transferred to
638 70% ethanol, and processed into paraffin. 5µm sections were cut and mounted onto
639 Superfrost Plus (Thermo-Fisher Scientific). Detection of Mouse Gdf15 was
640 performed on FFPE sections using Advanced Cell Diagnostics (ACD) RNAscope®
641 2.5 LS Reagent Kit-RED (Cat No. 322150) and RNAscope® LS 2.5 Probe Mm-
642 Gdf15-O1 (Cat No. 442948) (ACD, Hayward, CA, USA). Briefly, sections were baked
643 for 1 hour at 60°C before loading onto a Bond RX instrument (Leica Biosystems).
644 Slides were deparaffinized and rehydrated on board before pre-treatments using
645 Epitope Retrieval Solution 2 (Cat No. AR9640, Leica Biosystems) at 95°C for 15
646 minutes, and ACD Enzyme from the LS Reagent kit at 40°C for 15 minutes. Probe
647 hybridisation and signal amplification was performed according to manufacturer’s
648 instructions. Fast red detection of mouse Gdf15 was performed on the Bond RX
649 using the Bond Polymer Refine Red Detection Kit (Leica Biosystems, Cat No.
650 DS9390) according to the ACD protocol. Slides were then counterstained with
651 haematoxylin, removed from the Bond RX and were heated at 60°C for 1 hour,
652 dipped in Xylene and mounted using EcoMount Mounting Medium (Biocare Medical,
653 CA, USA. Cat No. EM897L).

654 Slides imaged on an automated slide scanning microscope (Axioscan Z1 and
655 Hamamatsu orca flash 4.0 V3 camera) using a 20x objective with a numerical
656 aperture of 0.8. Hybridisation specificity was confirmed by the absence of staining in
657 *Gdf15*^{-/-} mice.

658 RNA extraction was carried out with approximately 100mg of tissue in 1ml Qiazol
659 Lysis Reagent (Qiagen 793061) using Lysing Matrix D homogenisation tube and
660 Fastprep 24 Homogeniser (MP Biomedicals) and Qiagen RNeasy Mini kit (Cat no
661 74106) with DNase1 treatment following manufacturers' protocols. 500ng of RNA
662 was used to generate cDNA using Promega M-MLV reverse transcriptase followed
663 by TaqMan qPCR in triplicates for GDF15. Samples were normalised to Act B.
664 TaqMan Probes: Mm00442228 m1 GDF15, Mm02619580_g1 Act B, TaqMan;2X
665 universal PCR Master mix (Applied Biosystems Thermo Fisher 4318157);
666 QuantStudio 7 Flex Real time PCR system (Applied Biosystems Life Technologies)

667 **Mouse study 9. Acute phenformin study in standard chow-fed wild type**
668 **animals.**

669 Male C57BL6/J mice aged 14 weeks with supplier, protocol and methods as study 2,
670 except phenformin (Sigma PHR1573-500mg) used instead of metformin.

671 **Organoid studies.**

672 Duodenal and ileal mouse organoid line generation, maintenance and 2D culture
673 was performed as previously described³⁵. CHOP null mice were kind gift of Dr Jane
674 Goodall (University of Cambridge), with line from Jackson Laboratory, Maine
675 (B6.129S(Cg)-Ddit3tm2.1Dron/J, Stock No: 005530) Human rectal organoids
676 (experiments approved by the Research Ethics Committee under license number
677 09/H0308/24) were generated from fresh surgical specimens (Tissue Bank

678 Addenbrooke's Hospital (Cambridge, UK)) following a modified protocol^{35,36}. Briefly
679 rectal tissue was chopped into 5mm fragments and incubated in 30 mM EDTA for
680 3x10mins, with tissue shaken in PBS after each EDTA treatment to release intestinal
681 crypts. The isolated crypts were then further digested using TrypLE (Life
682 Technologies) for 5 mins at 37⁰C to generate small cell clusters. These were then
683 seeded into basement membrane extract (BME, R&D technology), with 20 µl domes
684 polymerised in multiwell (48) dishes for 30-60 mins at 37⁰C. Organoid medium (Sato
685 et al 2011) was then overlaid and changed 3 times per week. Human organoids were
686 passaged every 14-21 days using TrypLE digestion for 15 mins at 37⁰C, followed by
687 mechanical shearing with rigorous pipetting to breakup organoids into small clusters
688 which were then seeded as before in BME. For transwell experiments TrypLE
689 digested organoids were seeded onto matrigel (Corning) coated (2% for 60 mins at
690 37⁰C) polyethylene Terephthalate cell culture inserts, pore size 0.3 µm (Falcon) in
691 organoid medium supplemented with Y-27632 (R&D technology). Organoids were
692 observed through the transparent cell inserts to ensure 2D culture formation
693 (allowing apical cell access for drug treatments). Medium was changed after 2 days
694 and then switched on day 3 to a differentiation medium with wnt3A conditioned
695 medium reduced to 10% and SB202190 / nicotinamide omitted from culture for 5
696 days.

697 For GDF 15 secretion experiments 2D cultured organoid cells were treated for 24 hrs
698 with indicated drugs, with medium then collected and GDF15 measured at the Core
699 Biochemical Assay Laboratory (Cambridge) using the human or mouse GDF15
700 assay kit as outlined in CAMERA human study and mouse study 2 above.

701 RNA was extracted using TRI reagent (Sigma), with any contaminated DNA
702 eliminated using DNA free removal kit (Invitrogen). Purified RNA was then reverse

703 transcribed using superscript II (Invitrogen) as per manufacturer's protocol. RT-
704 qPCR was performed on a QuantStudio 7 (Applied Biosystems) using Fast Taqman
705 mastermix and the following probes (Applied Biosystems); Human GDF15
706 (Hs00171132_m1), Human ACTB (Hs01060665_g1). Gene expression was
707 measured relative to β -actin in the same sample using the Δ Ct method, with fold (cf.
708 control) shown for each experiment.

709 **Hepatocyte studies.**

710 **Primary mouse hepatocyte isolation and culture.**

711 Hepatocytes from 8-12 week old C57B6J male mice were isolated by retrograde,
712 non-recirculating in situ collagenase liver perfusion. In brief: livers were perfused with
713 modified Hanks medium without calcium (NaCl- 8.0 g/L; KCl- 0.4 g/L; MgSO₄.7H₂O-
714 0.2 g/L; Na₂HPO₄.2H₂O- 0.12 g/L; KH₂PO₄- 0.12 g/L; Hepes- 3 g/L; EGTA- 0.342
715 g/L; BSA- 0.05 g/L) followed by digestion with perfusion media supplemented with
716 calcium (CaCl₂.2H₂O- 0.585 g/L) and 0.5mg/ml of collagenase IV (Sigma, C5138).
717 The digested liver was removed and washed using chilled DMEM:F12 (Sigma)
718 medium containing 2 mM L-glutamine, 10 % FBS, 1% penicillin/streptomycin
719 (Invitrogen). Viable cells were harvested by Percoll (Sigma) gradient. The final pellet
720 was resuspended in the same DMEM:F12 media. Cell viability was greater than
721 90%. Hepatocytes were plated onto primaria plates (Corning). Hepatocytes were
722 allowed to recover and attach for 4-6 hr before replacement of the medium overnight
723 prior to stress treatments the following day for the times and concentrations
724 indicated.

725 **Generation and culture of iPSC derived human hepatocytes.**

726 The human induced pluripotent cell (hiPSC) line A1ATDR/R used in this work was
727 derived as previously described^{37,38} under approval by the regional research ethics
728 committee (reference number 08/H0311/201). hiPSCs were maintained in Essential
729 8 chemically defined media³⁹ supplemented with 2ng/ml Tgf- β (R&D) and 25ng/ml
730 FGF2 (R&D), and cultured on plates coated with 10 μ g/ml Vitronectin XFTM
731 (STEMCELL Technologies). Colonies were regularly passaged by short-term
732 incubation with 0.5mM EDTA in PBS. For hepatocyte differentiation, colonies were
733 dissociated into single cells following incubation with StemPro™ Accutase™ Cell
734 Dissociation Reagent (Gibco) for 5 minutes at 37°C. Single cell suspensions were
735 seeded on plates coated with 10 μ g/ml Vitronectin XFTM (STEMCELL Technologies)
736 in maintenance media supplemented with 10 μ M ROCK Inhibitor Y-27632
737 (Selleckchem) and grown for up to 72h prior to differentiation. Hepatocytes were
738 differentiated as previously reported⁴⁰, with minor modifications as listed. Briefly,
739 following endoderm differentiation, anterior foregut specification was achieved after 5
740 days of culture with RPMI-B27 differentiation media supplemented with 50ng/ml
741 Activin A (R&D)⁴⁰. Foregut cells were further differentiated into hepatocytes with
742 HepatoZYME-SFM (Gibco) supplemented with 2mM L-glutamine (Gibco), 1%
743 penicillin-streptomycin (Gibco), 2% non-essential amino acids (Gibco), 2%
744 chemically defined lipids (Gibco), 14 μ g/ml of insulin (Roche), 30 μ g/ml of transferrin
745 (Roche), 50 ng/ml hepatocyte growth factor (R&D), and 20 ng/ml oncostatin M
746 (R&D), for up to 27 days.

747

748 **Cellular studies on integrated stress response.**

749 **Chemicals and Reagents.**

750 Tunicamycin and ISRIB were purchased from Sigma-Aldrich. Metformin and
751 Phenformin was purchased from Cayman Chemicals and GSK2606414 from
752 Calbiochem. The antibody for GDF15 and CHOP (sc-7351) were obtained from
753 Santa Cruz. Phospho S51 EIF2 α (ab32157) and Calnexin (ab75801) were
754 purchased from Abcam. The antibody for ATF4 was a kind gift from Dr David Ron
755 (CIMR, Cambridge).

756 **Eukaryotic cell lines and treatments.**

757 Mouse embryonic fibroblast (MEF) cells lines were obtained from David Ron
758 (CIMR/IMS, Cambridge) and maintained as previously described¹⁸. MEFs were
759 transfected with 30 nM control siRNA or a smartpool on-target plus siRNA for mouse
760 CHOP (Dharmacon - L-062068-00-0005) using Lipofectamine RNAi MAX
761 (Invitrogen) according to the manufacturer's instruction. 48 h post siRNA
762 transfection, cells were processed for RNA and protein expression analysis. All cells
763 were maintained at 37 °C in a humidified atmosphere of 5 % CO₂ and seeded onto
764 6- or 12-well plates prior to stress treatments for the times and concentrations
765 indicated. Vehicle treatments (e.g. DMSO) were used for control cells when
766 appropriate.

767 **RNA isolation/cDNA synthesis/Q-PCR.**

768 Following treatments, cells were lysed with Buffer RLT (Qiagen) containing 1 % 2-
769 Mercaptoethanol and processed through a Qias shredder with total RNA extracted
770 using the RNeasy isolation kit according to manufacturer's instructions (Qiagen).
771 RNA concentration and quality was determined by Nanodrop. 400 ng - 500 ng of
772 total RNA was treated with DNase1 (ThermoFisher Scientific) and then converted to
773 cDNA using MMLV Reverse Transcriptase with random primers (Promega).

774 Quantitative RT-PCR was carried out with either TaqMan™ Universal PCR Master
775 Mix or SYBR Green PCR master mix on the QuantStudio 7 Flex Real time PCR
776 system (Applied Biosystems). All reactions were carried out in either duplicate or
777 triplicate and Ct values were obtained. Relative differences in the gene expression
778 were normalized to expression levels of housekeeping genes, HPRT or GAPDH for
779 cell analysis, using the standard curve method. Primers used for this study: mouse
780 GDF15 (Mm00442228_m1 – ThermoFisher Scientific), human GDF15
781 (Hs00171132_m1 - ThermoFisher Scientific), human GAPDH (Hs02758991_g1 –
782 ThermoFisher Scientific), mouse HPRT (Forward – AGCCTAAGATGAGCGCAAGT,
783 reverse - GGCCACAGGACTAGAACACC)

784 **Immunoblotting.**

785 Following treatments, cells were washed twice with ice cold D-PBS and proteins
786 harvested using RIPA buffer supplemented with cOmplete protease and PhosStop
787 inhibitors (Sigma). The lysates were cleared by centrifugation at 13 000 rpm for 15
788 min at 4 °C, and protein concentration determined by a Bio-Rad DC protein assay.
789 Typically, 20-30 µg of protein lysates were denatured in NuPAGE 4× LDS sample
790 buffer and resolved on NuPage 4-12 % Bis-Tris gels (Invitrogen) and the proteins
791 transferred by iBlot (Invitrogen) onto nitrocellulose membranes. The membranes
792 were blocked with 5 % nonfat dry milk or 5 % BSA (Sigma) for 1 h at room
793 temperature and incubated with the antibodies described in the reagents section.
794 Following a 16 h incubation at 4 °C, all membranes were washed five times in Tris-
795 buffered saline-0.1% Tween-20 prior to incubation with horseradish peroxidase
796 (HRP)-conjugated anti-rabbit immunoglobulin G (IgG), HRP-conjugated anti-mouse
797 IgG (Cell Signalling Technologies). The bands were visualized using Immobilon

798 Western Chemiluminescent HRP Substrate (Millipore). All images were acquired on
799 the ImageQuant LAS 4000 (GE Healthcare).

800 **Statistical analyses.**

801 CAMERA data were analysed using a mixed linear model with restricted maximum
802 likelihood to investigate the metformin effect on GDF-15. This is analogous to
803 conducting a repeated measures ANOVA, but is a more flexible analysis and allows
804 for missing observations within subject. The 0-18 months difference in weight and
805 GDF15 correlation was tested using Spearman's coefficient. CAMERA data were
806 analysed using STATA version 15.1.

807 Other statistical analyses were performed using Prism 7 and Prism 8, using
808 unpaired 2 tailed t-tests , or 2-way ANOVA, with multiple comparison adjustment by
809 Tukey's or Sidak's test. Metabolic rate was determined using ANCOVA with energy
810 expenditure as the dependent variable, body weight as a covariate and treatment as
811 a fixed factor. ANCOVA and analyses of glucose and insulin tolerance testing in
812 mice were performed using SPSS 25 (IBM).

813

814

815 **Data availability.**

816 The data that support the findings of this study are available from the corresponding
817 authors upon request. The CAMERA trial dataset is held at the University of
818 Glasgow and is available on request from the investigators subject to a signed
819 agreement operating within the confines of the original ethics application.

820

- 822 30 Skarnes, W. C. et al. A conditional knockout resource for the genome-wide study of mouse
823 gene function. *Nature* 474, 337-342, doi:10.1038/nature10163 (2011).
- 824 31 Bradley, A. et al. The mammalian gene function resource: the International Knockout Mouse
825 Consortium. *Mamm Genome* 23, 580-586, doi:10.1007/s00335-012-9422-2 (2012).
- 826 32 Pettitt, S. J. et al. Agouti C57BL/6N embryonic stem cells for mouse genetic resources. *Nat*
827 *Methods* 6, 493-495, doi:10.1038/nmeth.1342 (2009).
- 828 33 McNeilly, A. D., Williamson, R., Balfour, D. J., Stewart, C. A. & Sutherland, C. A high-fat-diet-
829 induced cognitive deficit in rats that is not prevented by improving insulin sensitivity with
830 metformin. *Diabetologia* 55, 3061-3070, doi:10.1007/s00125-012-2686-y (2012).
- 831 34 Ortega-Cava, C. F. et al. Strategic compartmentalization of Toll-like receptor 4 in the mouse
832 gut. *J Immunol* 170, 3977-3985, doi:10.4049/jimmunol.170.8.3977 (2003).
- 833 35 Goldspink, D. A. et al. Mechanistic insights into the detection of free fatty and bile acids by
834 ileal glucagon-like peptide-1 secreting cells. *Mol Metab* 7, 90-101,
835 doi:10.1016/j.molmet.2017.11.005 (2018).
- 836 36 Sato, T. et al. Long-term expansion of epithelial organoids from human colon, adenoma,
837 adenocarcinoma, and Barrett's epithelium. *Gastroenterology* 141, 1762-1772,
838 doi:10.1053/j.gastro.2011.07.050 (2011).
- 839 37 Rashid, S. T. et al. Modeling inherited metabolic disorders of the liver using human induced
840 pluripotent stem cells. *J Clin Invest* 120, 3127-3136, doi:10.1172/JCI43122 (2010).
- 841 38 Yusa, K. et al. Targeted gene correction of alpha1-antitrypsin deficiency in induced
842 pluripotent stem cells. *Nature* 478, 391-394, doi:10.1038/nature10424 (2011).
- 843 39 Chen, G. et al. Chemically defined conditions for human iPSC derivation and culture. *Nat*
844 *Methods* 8, 424-429, doi:10.1038/nmeth.1593 (2011).
- 845 40 Hannan, N. R., Segeritz, C. P., Touboul, T. & Vallier, L. Production of hepatocyte-like cells
846 from human pluripotent stem cells. *Nat Protoc* 8, 430-437 (2013).

847

848

849

850

851

852 Acknowledgments.

853 CAMERA trial funded by a project grant from the Chief Scientist Office, Scotland

854 (CZB/4/613).D.P. supported by a University of Oxford British Heart Foundation

855 Centre of Research Excellence Senior Transition Fellowship (RE/13/1/30181).

856 N.S. and P.W. acknowledge support from BHF Centre of Excellence award

857 (COE/RE/18/6/34217).The authors would like to thank Peter Barker, Keith Burling

858 and other members of the Cambridge Biochemical Assay Laboratory (CBAL) .This

859 project is supported by the National Institute for Health Research (NIHR) Cambridge

860 Biomedical Research Centre. The views expressed are those of the authors and not

861 necessarily those of the NIHR or the Department of Health and Social Care. A.P.C.,

862 D.Rimington, J.T., I.C., Y.C.L.T. and G.S.H.Y. are supported by the Medical
863 Research Council (MRC Metabolic Diseases Unit [MC_UU_00014/1]).
864 Mouse studies in Cambridge supported by Sarah Grocott and the Disease Model
865 Core, with pathology support from James Warner and Histopathology Core (MRC
866 Metabolic Diseases Unit (MC_UU_00014/5) and Wellcome Trust Strategic Award
867 (100574/Z/12/Z).D.B.S. and S.O'R. are supported by the Wellcome Trust (WT
868 107064 and WT 095515/Z/11/Z), the MRC Metabolic Disease Unit
869 (MC_UU_00014/1), and The National Institute for Health Research (NIHR)
870 Cambridge Biomedical Research Centre and NIHR Rare Disease Translational
871 Research Collaboration. We thank Julia Jones and other members of Histopathology
872 and ISH Core Facility, Cancer Research UK Cambridge Institute, University of
873 Cambridge, Li Ka Shing Centre, Robinson Way, Cambridge CB2 0RE, UK.D. Ron is
874 supported by a Wellcome Trust Principal Research Fellowship (Wellcome
875 200848/Z/16/Z) and a Wellcome Trust Strategic Award to the Cambridge Institute for
876 Medical Research (Wellcome 100140). A.V.-P., S.R.-C. and S.V. are supported by
877 the BHF (RG/18/7/33636) and MRC (MC_UU_00014/2).A.M. is supported by a
878 studentship from the Experimental Medicine Training Initiative/AstraZeneca.R.A.T.
879 and L.V. are supported by ERC advanced grant NewChol and core support from the
880 Wellcome Trust and Medical Research Council to the Wellcome–Medical Research
881 Council Cambridge Stem Cell Institute.M.Y., D.A.G., E.M., F.M.G. and F.R. are
882 supported by the MRC (MC_UU_00014/3) and Wellcome Trust (106262/Z/14/Z and
883 106263/Z/14/Z). M.Y. is supported by a BBSRC-DTP studentship. A.R.K., R.R.E.
884 and K.S.N. supported by NIH Grants R21 AG60139, UL1 TR000135 and
885 T32DK007352 and acknowledge Katherine Klaus for technical assistance. N.J.W. is

886 supported by the MRC (MC_UU_12015/1) and is an NIHR Senior Investigator. We
887 acknowledge Jian'an Luan for statistical assistance.

888 CHOP null mice were kind gift of Dr Jane Goodall (University of Cambridge).

889

890 **Author Contributions.**

891

892 Overall conceptualization of studies included in this body of work by A.P.C., N.S.,

893 D.B.S., B.B.A. and S.O'R. These authors contributed equally to this work.

894 A.P.C., M.C., P.T., D.Rimmington, I.C. and Y.C.L.T. designed, managed, performed

895 and analysed data from mouse experiments. S.V. designed experiments and

896 analysed data. A.M. and G.S.H.Y. contributed to conceptualisation of experiments

897 and data analysis. J.T. performed ISH experiments. S.P. designed, managed and

898 performed cell based assays along with E.L.M., S.R.C., R.A.T., H.P.H., A.V-P., L.V.

899 and D.Ron. J.T.J.H. undertook measurement of serum metformin levels .M.Y.,

900 D.A.G., F.M.G., F.R. designed, performed and analysed organoid experiments.

901 A.R.K., R.R.E. and K.S.N. designed and performed short term metformin studies in

902 humans. N.J.W undertook analysis of Ely Study Cohort. P.W., D.P. and N.S.

903 designed, analysed and interpreted data arising from the CAMERA study. A.P.C.,

904 D.B.S., B.B.A. and S.O'R. wrote the paper, which was reviewed and edited by all the

905 authors.

906

907 **Author information.**

908 P. W. has received grant support from Roche Diagnostics, AstraZeneca, and

909 Boehringer Ingelheim. N.S. has consulted for AstraZeneca, Boehringer Ingelheim, Eli

910 Lilly, Napp, Novo Nordisk and Sanofi, and received grant support from Boehringer

911 Ingelheim. M.C., P.T. and B.B.A. are or were employees of NGM

912 Biopharmaceuticals and may hold NGM stock or stock options. F.R. and F.M.G.
913 have received support from AstraZeneca and Eli Lilly. F.M.G. has provided
914 remunerated consultancy services to Kallyope. S.O'R has provided remunerated
915 consultancy services to Pfizer, AstraZeneca, Novo-Nordisk and ERX
916 Pharmaceuticals. **All other authors declare no competing financial interests.**

917 **Materials and correspondence.**

918 All requests for materials and correspondence A.P.C. (apc36@cam.ac.uk) and
919 S.O'R (so104@medschl.cam.ac.uk).

920
921

922

923 **Extended Data Figures Legends.**

924 **Extended Data Figure 1. Expanded CAMERA data set.**

925 **a**, Linear association between change in body weight and change in plasma GDF15
926 between 0 and 18 months among metformin treated participants (n=74, Spearman
927 correlation $r=-0.26$, two-sided $p=0.024$). Red line is linear regression slope, and grey
928 area is 95% confidence interval for slope.

929 **b**, Absolute and relative differences in plasma GDF15 concentration between
930 metformin and placebo groups at each time point (total 625 observations in 173
931 participants).

932 **c,d**, Individual measures of plasma GDF15 levels in placebo group (c) and
933 metformin group (d) over time.

934 **e**, Plasma GDF15 concentration (95%CI) in overweight or obese non-diabetic
935 participants with known cardiovascular disease randomised to metformin or placebo
936 in CAMERA; modelled using a mixed linear model as per Figure 1 and grouped as
937 "all participants" and "all participants not reporting diarrhoea and vomiting". Model
938 includes all participants

939

940 **Extended Data Figure 2. Effect of single oral dose of metformin in chow fed**
941 **mice.**

942 Serum GDF15 levels in male mice measured 2, 4, or 8 hours after a single gavage
943 dose of metformin (300mg/kg). **a**, mice *ad libitum* overnight fed prior to gavage. **b**,

944 mice fasted for 12 hour prior to gavage. Data are mean ± SEM (**a**; n=6/group, **b**; n=
945 4/group); P by 2-way ANOVA with Tukeys correction for multiple comparisons.

946

947 **Extended Data Figure 3. Body weight changes with metformin treatment in**
948 **mice with disrupted GDF15-GFRAL signalling.**

949 **a**, Absolute body weight in *Gdf15*^{+/+} and *Gdf15*^{-/-} mice on a high-fat diet treated with
950 metformin (300mg/kg/day) for 11 days, mice as **Figure 2a**. Data are mean ± SEM, P
951 by 2-way ANOVA with Tukey's correction for multiple comparisons.

952 **b**, Absolute body weight in high fat diet fed *Gfral*^{+/+} and *Gfral*^{-/-} mice given oral
953 dose of metformin (300mg/kg) once daily for 11 days, mice as **Figure 2c**. Data are
954 mean ± SEM.

955 **c**, Absolute body weight of metformin-treated, obese mice dosed with an anti-GFRAL
956 antagonist antibody or with control IgG weekly for 5 weeks starting 4 weeks after
957 initial metformin exposure, mice as **Figure 2d**. Data are mean ± SEM. P by 2-way
958 ANOVA with Tukey's correction for multiple comparisons.

959

960 **Extended Data Figure 4. Response of high fat diet fed *Gdf15*^{-/-} and *Gfral*^{-/-} mice**
961 **to metformin.**

962 **a**, Circulating GDF15 levels in high fat diet fed *Gdf15*^{+/+} and *Gdf15*^{-/-} mice given
963 oral dose of metformin (300mg/kg) once daily for 11 days. Data are mean ± SEM,
964 mice as **Figure 2a**. All samples from *Gdf15*^{-/-} were below lower limit of assay (<
965 2pg/ml), P value by 2-way ANOVA with Tukey's correction for multiple comparisons.

966 **b**, Circulating GDF15 levels in high fat diet fed *Gfral*^{+/+} and *Gfral*^{-/-} mice given oral
967 dose of metformin (300mg/kg) once daily for 11 days. Data are mean ± SEM, mice
968 as **Figure 2c**, P by 2-way ANOVA with Tukey's correction for multiple comparisons.

969 **c**, Cumulative food intake in high fat diet fed *Gfral*^{+/+} and *Gfral*^{-/-} mice on a high fat
970 diet given oral dose of metformin (300mg/kg) once daily for 11 days. Data are mean
971 ± SEM, mice as **Figure 2c**, non-significant difference vehicle vs metformin by 2W
972 ANOVA.

973 **d**, Fat mass (left panel) and lean mass (right panel) in metformin-treated obese
974 mice dosed with an anti-GFRAL antagonist antibody, weekly for 5 weeks, starting 4
975 weeks after initial metformin exposure (mice as **Figure 2d**). Body composition was
976 measured using MRI after 4 weeks of metformin exposure, prior to receiving anti-
977 GFRAL (week 4), after 6 weeks of metformin exposure and 2 weeks after receiving
978 anti-GFRAL (week 6) and after 9 weeks of metformin exposure and 5 weeks after
979 receiving anti-GFRAL (week 9). Data are mean ± SEM (n=7 Vehicle + control IgG
980 and Metformin + anti – GFRAL; n=8 other groups); P by 2-way ANOVA with Tukey's
981 correction for multiple comparisons.

982

983 **Extended Data Figure 5. Response of second, independent cohort of high-fat**
984 **diet fed *Gdf15*^{+/+} and *Gdf15*^{-/-} mice to metformin.**

985 **a,b,c**, Percentage change in body weight (**a**), absolute body weight (**b**) and
986 cumulative food intake (**c**) in *Gdf15*^{+/+} and *Gdf15*^{-/-} mice on a high-fat diet treated
987 with metformin (300mg/kg/day) for 11 days. Data are mean ± SEM (n=6/group,
988 except *Gdf15*^{-/-} vehicle= 7), P by 2-way ANOVA with Tukey's correction for multiple
989 comparisons.

990 **d**, Circulating metformin levels in mice 6 hrs after final dose of metformin on day 11.
991 Data are mean ± SEM (n=6/group, except *Gdf15*^{+/+} vehicle= 4, *Gdf15*^{-/-} vehicle=
992 7), P by 2-way ANOVA with Tukey's correction for multiple comparisons.

993 **Extended Data Figure 6. Glucose, insulin and GDF15 response to metformin.**

994 **a**, Fasting glucose from OGTT as **Figure 3e** and **3f**. ANOVA analysis, effect of
995 antibody p= 0.028, effect of metformin p= 0.271, interaction of antibody and
996 metformin p 0.707.

997 **b**, Circulating GDF15 in mice undergoing ipGTT post single dose metformin as
998 **Figure 3 k** and **3l**. P by 2-way ANOVA with Tukey's correction for multiple
999 comparisons.

1000 **c,d**, Fasting glucose (**c**) and fasting insulin (**d**) at time 0 of ipGTT as **Figure 3 k** and
1001 **3l**, non-significant by 2-way ANOVA.

1002 **e**, AUC analysis of glucose levels as in Figure 3k and l. P by 2-way ANOVA, effect of
1003 genotype p= 0.392, interaction of genotype and metformin p= 0.883.

1004 **f**, Circulating GDF15 levels in high-fat diet fed *Gdf15*^{+/+} mice after single oral dose
1005 of metformin (600mg/kg). Samples were collected 6 hours after dosing, data are
1006 mean ± SEM, (n=7/group), P value (95% confidence interval) by two tailed t-test.
1007

1008 **Extended Data Figure 7. a**, Representative images from the mouse with circulating
1009 GDF15 level closest to group median shown in Fig4b with images from other regions
1010 of the gut and from liver. **b**, In situ hybridization for *Gdf15* mRNA expression (red
1011 spots) in colon. Tissue collected from high-fat fed wild type mice, 6 hrs after single
1012 dose of oral metformin (600mg/kg) (right side, red box, m1-m7) or vehicle gavage (
1013 left side, blue box, v1-v7), n=7/group, mice as **Figure 4**.

1014 **Extended Data Figure 8. Analysis of *Gdf15* mRNA expression (normalised to**
1015 **expression levels of *ActB*) in tissue from high fat diet fed *Gdf15*^{+/+} mice.**

1016 Metformin dose (300mg/kg) once daily for 11 days (see **Figure 2a**). Data are mean
1017 ± SEM, n=6 metformin, n=7 vehicle, P value (95% confidence interval) by two tailed
1018 t-test.

1019 **Extended Data Figure 9. Hepatic GDF15 response to biguanides.**

1020 **a,b**, *Gdf15* mRNA expression in (**a**) primary mouse hepatocytes or (**b**) human iPSC
1021 derived hepatocytes treated with vehicle control (Con) or metformin for 6 h. mRNA
1022 expression is presented as fold expression relative to control treatment (set at 1),
1023 normalised to *Hprt* and *GAPDH* gene in mouse and human cells, respectively. Data
1024 are expressed as mean ± SEM from four (**a**) and two (**b**) independent experiments. P

1025 value (95% confidence interval) by 1 way ANOVA with Tukey's correction for
1026 multiple comparisons.

1027 **c,d**, Circulating levels of GDF15 (**c**) and hepatic *Gdf15* mRNA expression (**d**)
1028 (normalised to $\beta 2$ microglobulin) in chow fed, wild type mice 4 hrs after single oral
1029 dose of phenformin (300mg/kg). Data are mean \pm SEM, n= 6/group, P value (95%
1030 confidence interval) by two tailed t-test.

1031 **e**, Representative image of in situ hybridization for *Gdf15* mRNA expression (red
1032 spots) of fixed liver tissue derived from animals treated as described in (**c**) and (**d**).

1033 **Extended 10. Role of the Integrated Stress Response (ISR) in biguanide-** 1034 **induced Gdf15 expression**

1035 **a,b**, mRNA levels in kidney (**a**) and colon (**b**) isolated from obese mice 24 hours after
1036 a single oral dose of metformin (600mg/kg). Data are mean \pm SEM (n=5/group). P
1037 values (95% confidence interval) by two tailed t-test. *Gdf15* mRNA fold induction 24
1038 hrs post metformin 600mgs/kg is positively correlated with CHOP mRNA induction in
1039 both kidney (**a**, right panel) and colon (**b**, right panel), black line= linear regression
1040 analysis.

1041 **c-g**, Immunoblot analysis of ISR components (**c**) and *Gdf* mRNA expression (**d**) in
1042 wild type MEFs (mouse embryonic fibroblasts) treated with vehicle control (Con),
1043 metformin (Met, 2 mM) or phenformin (Phen, 5 mM) or tunicamycin (Tn, 5 μ g/ml -
1044 used as a positive control) for 6 hrs. **e**, *Gdf15* mRNA expression in ATF4 knockout
1045 (KO) MEFs or (**f**) in control siRNA and CHOP siRNA transfected wild type MEFs
1046 treated with Tn or Phen for 6 hrs or (**g**) in wild type MEFs pre-treated for 1 h either
1047 with the PERK inhibitor GSK2606414 (GSK, 200 nM) or eIF2 α inhibitor ISRIB (ISR,
1048 100 nM) then co-treated with Phen for a further 6 hrs. mRNA expression is presented
1049 as fold-expression relative to its respective control treatment (set at 1) or phen
1050 treated samples (set as 100) with normalisation to *Hprt* gene expression. Data are
1051 expressed as mean \pm SEM from two for (**c**) and (**d**) and at least three independent
1052 experiments for (**e-g**). P value (95% confidence interval) by two tailed t-test relative
1053 to Phen treated control wild and control siRNA treated samples.

1054 **h**, GDF15 protein in supernatant of mouse derived 2D duodenal organoids treated
1055 with metformin in the absence or presence of ISRIB (1 μ M). Data are expressed as
1056 mean \pm SEM from two independent experiments. From each well, measurement of
1057 protein was at least in duplicate. P by 2 way ANOVA with Sidak's correction for
1058 multiple comparisons.

1059 **i**, GDF15 protein in supernatants of mouse-derived 2D duodenal organoids from wild
1060 type and CHOP null mice treated with metformin from two independent experiments
1061 From each well, measurement of protein was at least in duplicate. Data are mean \pm
1062 SEM, P value (95% confidence interval) by two-tailed t-test.

1063

1064

1065

1066

1067

1068

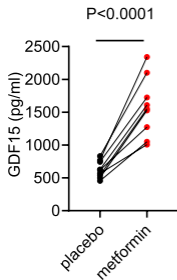
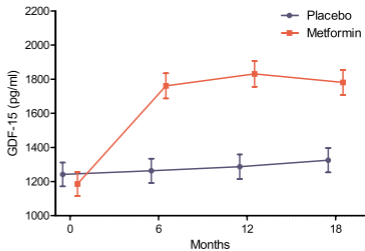
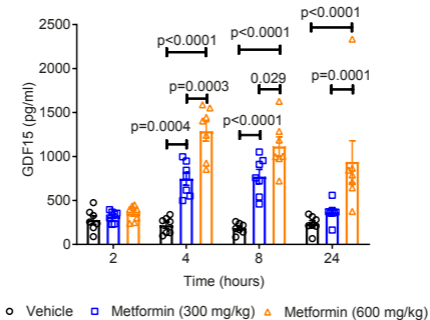
1069

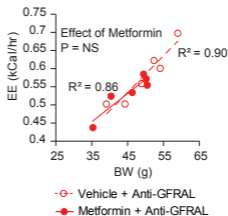
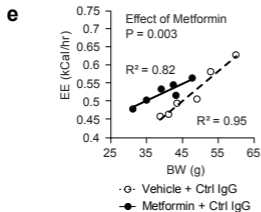
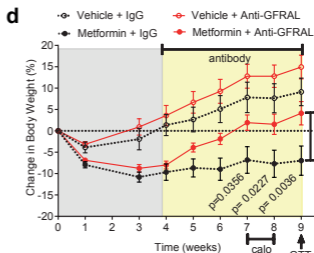
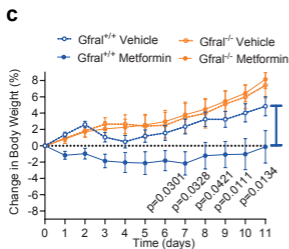
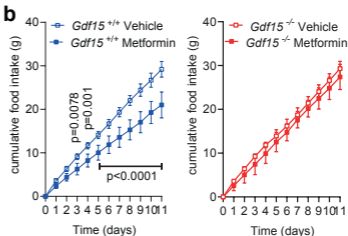
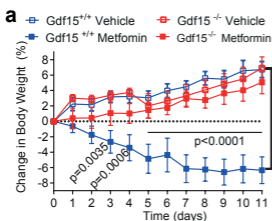
1070

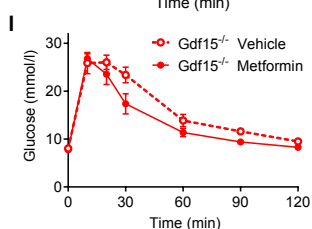
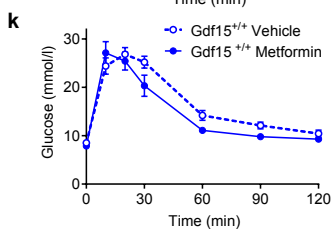
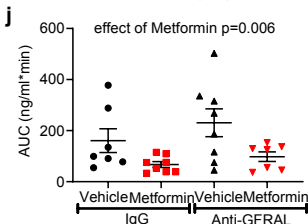
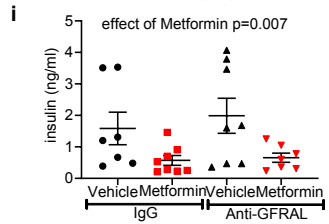
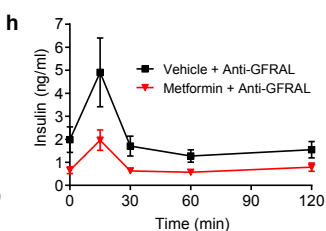
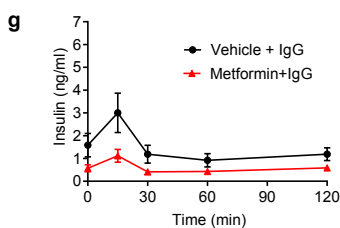
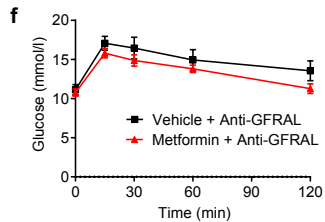
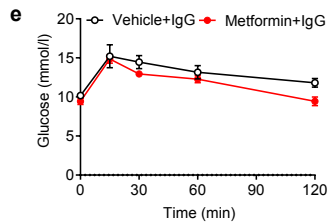
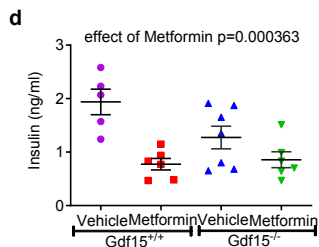
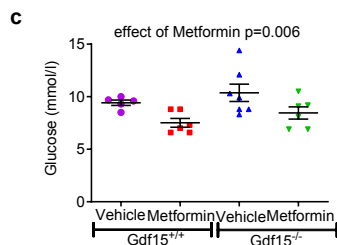
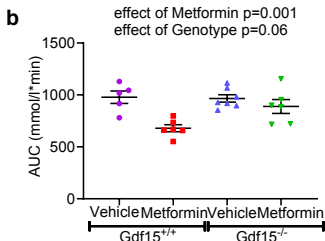
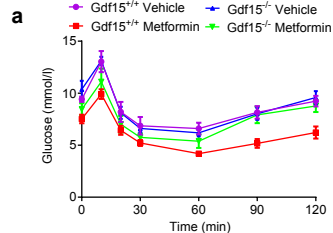
1071

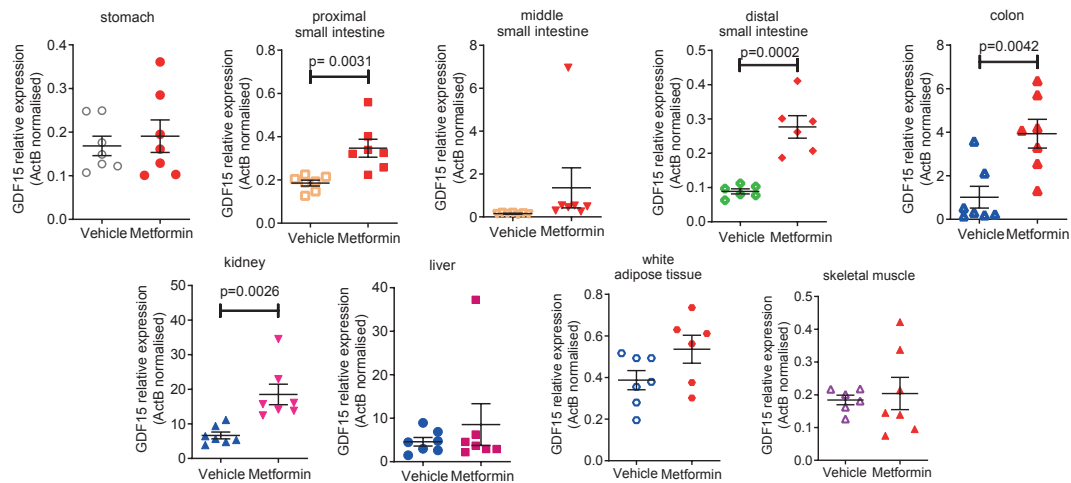
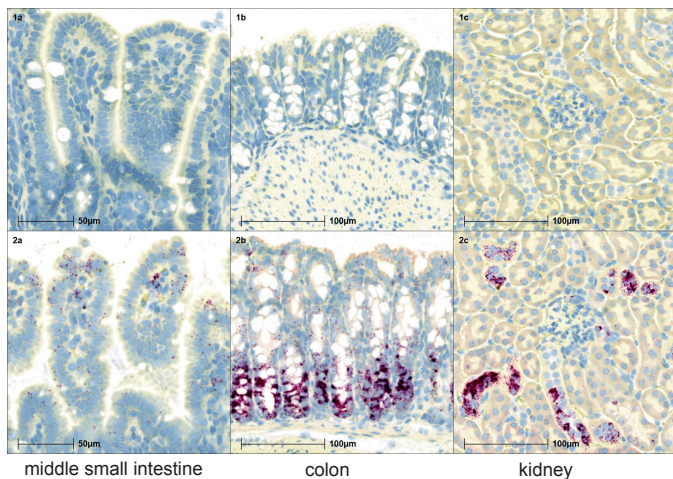
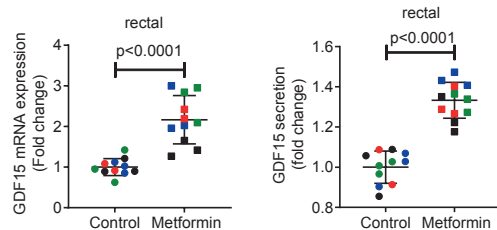
1072

1073

a**b****c**





a**b****c****d**